MIT Libraries | DSpace@MIT

MIT Open Access Articles

Pressure-induced spin-Peierls to incommensurate charge-density-wave transition in the ground state of TiOCl

The MIT Faculty has made this article openly available. ***Please share*** how this access benefits you. Your story matters.

Citation: Prodi, A. et al. "Pressure-induced spin-Peierls to incommensurate charge-density-wave transition in the ground state of TiOCl." Physical Review B 81.20 (2010): 201103. © 2010 The American Physical Society.

As Published: http://dx.doi.org/10.1103/PhysRevB.81.201103

Publisher: American Physical Society

Persistent URL: http://hdl.handle.net/1721.1/58735

Version: Final published version: final published article, as it appeared in a journal, conference proceedings, or other formally published context

Terms of Use: Article is made available in accordance with the publisher's policy and may be subject to US copyright law. Please refer to the publisher's site for terms of use.

Massachusetts Institute of Technology

PHYSICAL REVIEW B **81**, 201103(R) (2010)

Pressure-induced spin-Peierls to incommensurate charge-density-wave transition in the ground state of TiOCl

A. Prodi,[1,2] J. S. Helton,[1] Yejun Feng,[3] and Y. S. Lee[1]

[1]*Department of Physics, Massachusetts Institute of Technology, Cambridge, Massachusetts 02139, USA*

[2]*Center for Materials Science and Engineering, Massachusetts Institute of Technology, Cambridge, Massachusetts 02139, USA*

[3]*The Advanced Photon Source, Argonne National Laboratory, Argonne, Illinois 60439, USA*

(Received 24 March 2010; published 28 May 2010)

The ground state of the spin-Peierls system TiOCl was probed using synchrotron x-ray diffraction on a single-crystal sample at $T=6$ K. We tracked the evolution of the structural superlattice peaks associated with the dimerized ground state as a function of pressure. The dimerization along the b axis is rapidly suppressed in the vicinity of a first-order structural phase transition at $P_C=13.1(1)$ GPa. The high-pressure phase is characterized by an incommensurate charge-density wave perpendicular to the original spin-chain direction. These results show that the electronic ground state undergoes a fundamental change in symmetry, indicating a significant change in the principal interactions.

DOI: 10.1103/PhysRevB.81.201103 PACS number(s): 78.70.Ck, 64.70.Tg, 74.62.Fj, 75.10.Pq

Low-dimensional quantum magnets display rich physics due to the interplay of spin, lattice, orbital, and charge degrees of freedom. As a well-known example, the spin-Peierls transition occurs when the presence of the spin-phonon coupling in spin-1/2 antiferromagnetic chains causes the formation of singlet pairs on structural dimers. Only a handful of physical systems have been identified with a spin-Peierls ground state, including several complex organic compounds[1] and the inorganic compound $CuGeO_3$ (Ref. 2). However, the latter material may not be a good realization of a conventional spin-Peierls system.[2–4] Recently, the inorganic material TiOCl has been shown to exhibit spin-Peierls physics.[5–9] The system is composed of chains of Ti ions which undergo successive transitions upon cooling to an incommensurate nearly dimerized state at $T_{C2}=92$ K and to a commensurate dimerized state at $T_{C1}=66$ K, respectively. The orthorhombic crystal structure of TiOCl, illustrated in Fig. 1, consists of bilayers of Ti and O atoms, separated by chlorine layers along the c axis. Within the a-b plane, $Ti^{3+}(3d^1, S=\frac{1}{2})$ ions form a buckled rectangular lattice where the dominant magnetic interaction is due to Ti-Ti direct exchange along the b direction. This gives rise to one-dimensional (1D) quantum spin chains along b, where the interchain interaction is frustrated. The geometry of the Ti ions is depicted in Fig. 1(b). The formation of a dimer state below $T_{C1}=66$ K involves a substantial displacement ($\delta=0.03b$) of Ti^{3+} ions along the chain direction, doubling the unit cell along the b axis with the appearance of superlattice reflections with wave vector $\mathbf{q}=(0,\frac{1}{2},0)$.[8,9] A key prediction of the conventional spin-Peierls theory[10] has been confirmed in TiOCl with the direct observation of the softening of the spin-Peierls active phonon at T_{C1} by means of inelastic x-ray scattering.[9]

Hydrostatic pressure has served as a key experimental tuning parameter in exploring the interconnection between different correlated electronic states. Rich phenomena driven by pressure in low-dimensional systems include commensurate-to-incommensurate transition in charge-density-wave dichalcogenides,[11–13] spin-Peierls to superconductivity transition in organic systems,[14] a hierarchical phase diagram in the spin-ladder compound NaV_2O_5,[15,16] and novel phase transitions in $CuGeO_3$.[17,18] Recent studies of TiOCl under pressure[19,20] have suggested that the system undergoes a metallization associated with changes in the crystal structure at pressures $P\sim16$ GPa. The interpretation of these results in terms of bandwidth-controlled Mott transition is still under debate.[21,22] Measurements of the electrical resistance under pressure show that TiOCl remains semiconducting up to 24 GPa, however, the energy gap indicates a critical pressure of ~13 GPa above which the electronic structure changes.[21] Currently, there are no measurements of how the dimerized spin-Peierls ground state is affected by increasing pressure through the critical pressure. Most previous experiments were carried out at room temperature and are not sensitive to the low-temperature ground state.

We report direct measurements of both the fundamental lattice and weaker superlattice structural reflections in TiOCl under pressure and at low temperatures using high-resolution x-ray diffraction on a single-crystal sample. We observed a sudden first-order structural phase transition and determined the transition pressure to be $P_C=13.1$ GPa. In addition, the

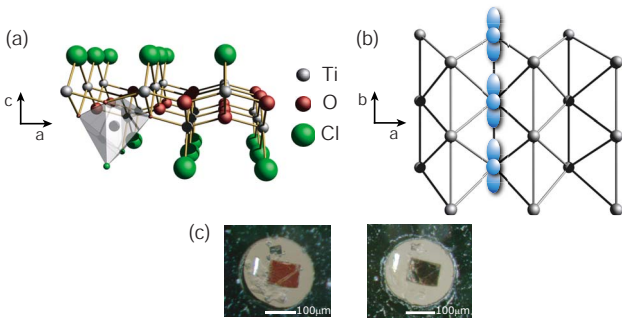

FIG. 1. (Color online) (a) Crystal structure of TiOCl viewed along the spin-chain direction. The Ti atoms are shown in gray. (b) Ti sublattice showing the orbital arrangement yielding chains along b in the low-pressure phase. (c) Micrograph of the TiOCl sample inside the diamond-anvil cell at room temperature, before (with $P<0.5$ GPa) and after (with $P\sim3$ GPa) the x-ray measurements. The silver pressure calibrant is visible at the left of the sample.

 ©2010 The American Physical Society

superlattice peaks indicate that the low-pressure (LP) spin-Peierls dimerization is significantly diminished at the phase boundary and disappears above P_C. In the high-pressure (HP) phase, the system orders with an incommensurate charge-density wave along the a-axis direction (perpendicular to the spin chains of the low-pressure phase). This new feature of the ground state points to either a change in the dimensionality of the high-pressure state or a significant change in the principal interactions.

Synchrotron x-ray diffraction experiments at high pressures and low temperatures were carried out at the 4-ID-D beamline of the Advanced Photon Source at Argonne National Laboratory. Incident x rays with energy 20 keV were selected using a Si(111) double monochromator and were focused onto the sample by Pd mirrors. A He-gas-driven membrane diamond-anvil cell was mounted on the cold finger of a closed-cycle cryostat to apply pressures up to 16 GPa with *in situ* tunability.[23,24] Measurements were performed by monotonically increasing the membrane pressure in small ($\sim$0.2 GPa) increments while at base temperature $T_0=6.0\pm0.5$ K. The cryostat was installed on the sample stage of a psi-circle diffractometer working in the vertical scattering geometry. The high collimation of both the incident and scattering x-ray paths, the large (>1 m) Rowland circle, and the use of a NaI point detector, yield high wave-vector resolution and efficient rejection of background scattering from the sample environment. Pressure was calibrated *in situ*[24] against the lattice constant of silver, determined from powder lines of a silver foil inside the pressure chamber.

Single crystals of TiOCl of 100 μm$\times$100 μm $\times$10 μm typical size and 0.3° mosaic spread were selected from batches grown by the vapor transport method.[5] A 4:1 methanol/ethanol mixture was used as the pressure-transmitting medium. The flaky, amber colored single crystal lay flat on the diamond culet when mounted, with the c-axis oriented along the loading axis. In the resulting (transmission) scattering geometry, diffraction peaks are easily accessible in the $L=0$ plane while information regarding the c-axis lattice constant can be accessed via $(H,0,L)$ reflections. In total, three fundamental Bragg [(200), (020), and (201)] and five superlattice reflections were observed as a function of pressure. We note that during the experiment, the width of one of the rocking scans increased under pressure from 0.3° at 0.8 Gpa to $\sim$5° at 12 GPa. This increased mosaic spread likely results from a slight crumpling of the thin crystal under pressure in the diamond-anvil cell. The crystal, however, remains intact, and the positions of the Bragg peaks and the relative intensities of the superlattice peaks can still provide important information, as we discuss below. We also note that the alcohol mixture has been proven to provide static pressure conditions with homogeneity better than $\Delta P=0.1$ GPa in this pressure and temperature range.[24]

We first display the measured TiOCl lattice parameters along all three axes as a function of pressure in the low-temperature spin-Peierls phase at $T=6$ K as shown in Fig. 2. The lattice parameters are normalized to their corresponding values measured at ambient pressure. The zero-pressure axial compressibilities, $\beta_{0,i}=a_{0,i}^{-1}(\partial a_i/\partial P)_{P=0}$, show a marked anisotropy with $\beta_{0,a}:\beta_{0,b}:\beta_{0,c}\approx 1:5.3:10$, $\beta_{0,a}=1.245(1)\times10^{-3}$ GPa^{-1}. A least-squares fit of the unit-cell volume to a Murnaghan equation of state[25] leads to a bulk modulus of $B_0=34$ GPa and $B_0'=8$ GPa. These values are consistent with the corresponding values reported from powder x-ray diffraction at room temperatures.[20] At $P=12.3$ GPa, we find $a=3.729(5)$ Å, $b=3.141(4)$ Å, and $c=7.27(22)$ Å as referred to the pseudo-orthorhombic setting.

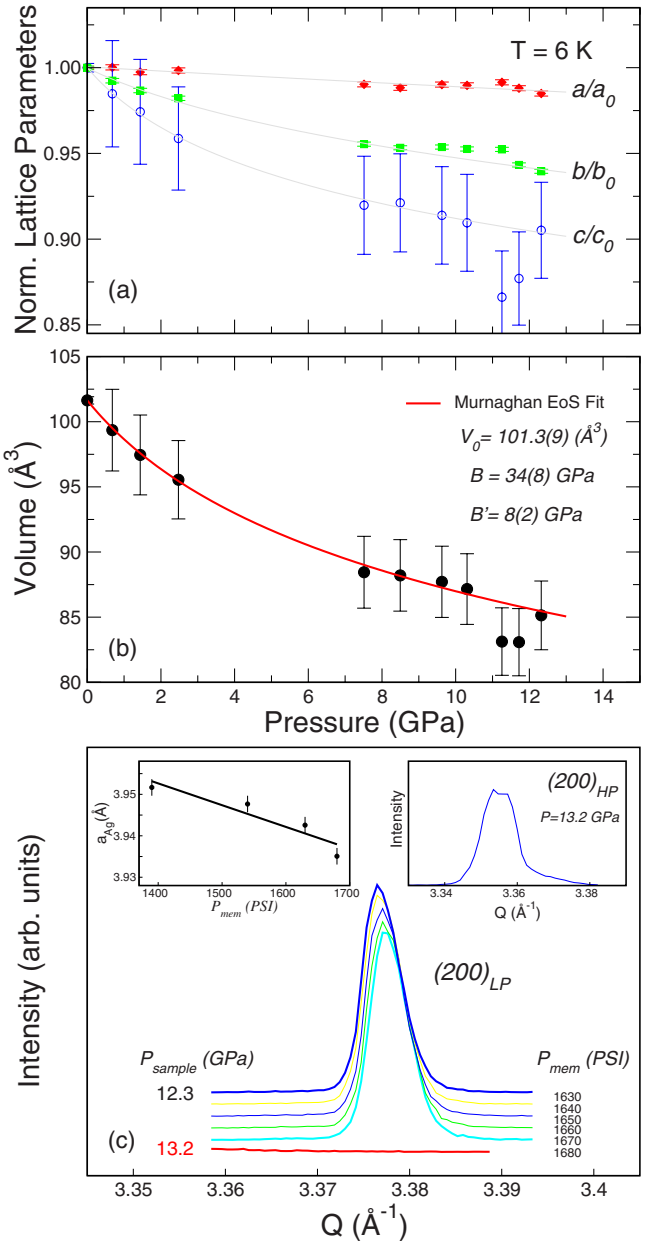

FIG. 2. (Color online) (a) Pressure dependence of the unit-cell parameters of TiOCl at $T=6$ K. (b) Low-temperature unit-cell volume with fit to a Murnaghan equation of state. (c) Measurements of the (200) fundamental Bragg reflection as the pressure is increased in fine steps. Left inset: the sample pressure measured by the Ag lattice constant is linear relative to the membrane load in this pressure range. Right inset: the (200) peak of the high-pressure phase, using pseudo-orthorhombic notation.

As shown in Fig. 2(c), a first-order structural transition is observed between LP and HP phases, indicated by the sud-

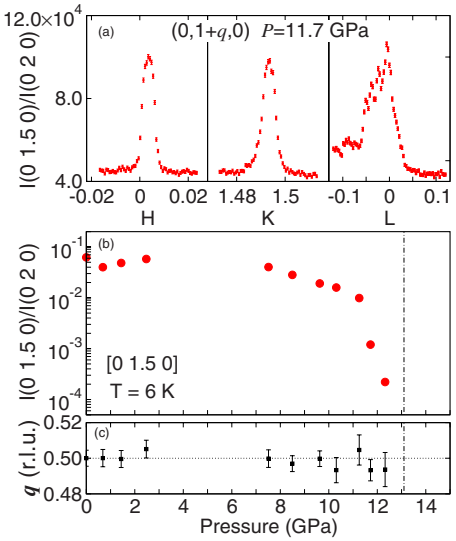

FIG. 3. (Color online) Pressure dependence of the $(0\ \frac{3}{2}\ 0)$ superlattice reflection of TiOCl at $T=6$ K. (a) Representative scans at 11.7 GPa; the intensity is scaled to the closest fundamental Bragg peak (0 2 0). (b) Intensity and (c) wave vector $\boldsymbol{q}$ of the structural superlattice as a function of pressure. The error bars for the intensity is smaller than symbol size while the error bars for $\boldsymbol{q}$ represent the fitted widths of the scans along K.

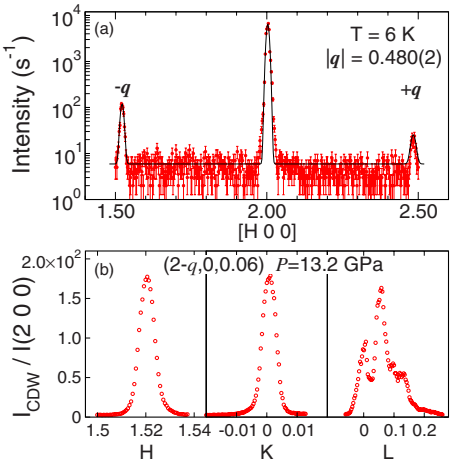

FIG. 4. (Color online) (a) Longitudinal scan along the $[H00]$ direction of the high-pressure phase of TiOCl at $T=6$ K. A new pair of superlattice peaks are observed around the (200) Bragg peak with incommensurate wave vector $q=0.48$. (b) Scans through the incommensurate $(2-q,0,0)$ peak along the H, K, and L directions, using pseudo-orthorhombic notation.

den disappearance of the $(200)_{\mathrm{LP}}$ reflection. A precise value of $P_c=13.1(1)$ GPa for the transition pressure can be obtained by finely stepping the membrane pressure and monitoring the (200) fundamental Bragg reflection. The left inset shows that the measured lattice constant of the Ag foil varies linearly with pressure in this range. Above P_c, three new peaks belonging to the high-pressure phase could be indexed as $(200)_{\mathrm{HP}}$, $(020)_{\mathrm{HP}}$, and $(201)_{\mathrm{HP}}$ again in a pseudo-orthorhombic unit cell setting with $a=3.746(11)$ Å, $b=3.150(8)$ Å, and $c=6.94(57)$ Å. It is interesting to note that the a lattice parameter *increases* from the low-pressure to high-pressure structures, a result predicted by recent *ab initio* calculations.[22] The volume strain associated with the transition is $V_s=(V_{\mathrm{HP}}-V_{\mathrm{LP}})/V_{\mathrm{LP}}=-0.0374$. After warming the cell to room temperature, visual inspection evidenced a color change in the sample. The dark brown color of the high-pressure sample is retained upon decompression down to 3 GPa (the color is similar to that observed in the "metallic" state at room temperature reported previously[19]). This large pressure hysteresis is striking, though some degree of hysteresis is expected for a first-order structural transition.

One of the main results of this work is the observation of the weak diffracted signal from the superlattice peaks at pressures above and below P_C. For pressures below P_C, we measured the (0,1.5,0) superlattice peak which reflects the dimerized structure of the spin-Peierls phase. The data are shown in Fig. 3. In panel (a), we show H, K, and L scans through the peak, where the intensity is normalized to that of the nearby (020) Bragg peak. Note that this superlattice peak (which is one of the most intense) is about three orders of magnitude less intense than the fundamental Bragg peak, hence it is difficult to observe in measurements on powder samples. The pressure dependence of the normalized intensity of the $(0\ \frac{3}{2}\ 0)$ superlattice reflection is shown in Fig. 3(b). The intensity remains relatively flat over a wide pressure range up to 11 GPa, then rapidly decreases over a pressure range of about 2 GPa prior to reaching P_C. The modulation wave vector $\boldsymbol{q}$, shown in panel (c), indicates that the periodic distortion remains commensurate with the lattice at all pressures (within alignment errors). We also find that the superlattice peak remains resolution limited, within the errors, at all pressures along H and K, indicating long-range order of the dimerized phase exists up to P_C. The other measured superlattice reflections (not shown) display similar behavior. Since the diffracted intensity is related to the modulation as $I\propto|\vec{Q}\cdot\vec{\delta}|^2$ and the largest contribution is due to the Ti atomic displacement along the b axis, we can estimate that the Ti-Ti dimerization amplitude δ is suppressed by at least a factor of 15 prior to reaching the first-order phase transition.

Interestingly, in the high-pressure phase, a new ground state emerges which is characterized by a pair of incommensurate superlattice peaks at (1.52, 0, 0) and (2.48, 0,0) as shown in Fig. 4. These peaks are near the commensurate positions $(2\pm0.5,0,0)$, and the incommensurate nature of this new structure can be clearly seen in the longitudinal scan of Fig. 4(a). We can describe this modulation of the high-pressure structure with a modulation vector $\boldsymbol{q}=(1-\varepsilon)\boldsymbol{a}^*/2$ and discommensuration $\varepsilon=0.02$. Surprisingly, instead of ordering along the b axis as in the spin-Peierls ground state, the new modulation vector is along the a axis, which is perpendicular to the low-pressure spin chain direction. This is in contrast to the incommensurate structure of TiOCl observed at ambient pressure for temperatures between $T=66$ and 93 K,[9,26] which centers around the $(0,2\pm0.5,0)$ position. We did not observe any superlattice diffraction intensity at $(0,2\pm0.5,0)$ in the high-pressure phase.

The stability of the spin-Peierls ground state results from the balance between gain in magnetic energy from the dimerization and the cost in elastic energy of the associated distortion. The competing terms are tuned simultaneously by pres-

sure while the reduction in interatomic distances upon compression always increases the elastic energy cost, the influence on the magnetic energy is more subtle through its dependence on the exchange J, the spin-phonon coupling constant, and on the soft phonon mode. Our results suggest that the balance holds until a threshold is reached near P_C and the dimerization is rapidly suppressed. A recent density matrix renormalization group study suggests that the dimerization amplitude δ is independent of $J_{a,c}/J_b$ for a wide range of the parameters.[27] In the high-pressure phase, the incommensurate structure along the a axis may originate from a Fermi-surface nesting of an itinerant electron state. A previous report using powder x-ray diffraction study claimed that a conventional Peierls dimerization exists along the b direction in the high-pressure phase at room temperature.[28] Our results show that this proposed state does not exist at $T=6$ K. If conventional Peierls physics is operative at high pressure, then the chain direction should have switched to the a direction. The slight incommensurability that we observe would be hard to explain in such a model. One possibility is that the dimensionality of the system may change from one-dimensional to quasi-two-dimensional when crossing from the insulating low-pressure phase to the more metallic high-pressure phase. Further work is needed to confirm the charge-density wave nature of the ground state, such as searching for thermodynamic signatures or Kohn anomalies.

In summary, by performing high-pressure x-ray scattering studies of a single-crystal sample of TiOCl at low temperatures, we directly observed the diminishment of the dimerized superlattice in the vicinity of the critical pressure P_C. The spin-Peierls dimerization along b does not survive above P_C. Above P_C, incommensurate superlattice peaks along the a direction are observed. We conclude that a charge-density wave exists in the ground state of the high-pressure phase.

We thank F. C. Chou, S. H. Shim, E. T. Abel and D. B. McWhan for fruitful discussions. The work at MIT was supported by the Department of Energy (DOE) under Grant No. DE-FG02-07ER46134. Use of the Advanced Photon Source at Argonne National Laboratory was supported by the DOE under Contract No. DE-AC02-06CH11357. This work used facilities supported in part by the NSF under Agreement No. DMR-0454672.

[1] I. S. Jacobs, J. W. Bray, H. R. Hart, L. V. Interrante, J. S. Kasper, G. D. Watkins, D. E. Prober, and J. C. Bonner, Phys. Rev. B **14**, 3036 (1976).
[2] M. Hase, I. Terasaki, and K. Uchinokura, Phys. Rev. Lett. **70**, 3651 (1993).
[3] J. Riera and A. Dobry, Phys. Rev. B **51**, 16098 (1995).
[4] L. P. Regnault, M. Aïn, B. Hennion, G. Dhalenne, and A. Revcolevschi, Phys. Rev. B **53**, 5579 (1996).
[5] A. Seidel, C. A. Marianetti, F. C. Chou, G. Ceder, and P. A. Lee, Phys. Rev. B **67**, 020405(R) (2003).
[6] V. Kataev, J. Baier, A. Möller, L. Jongen, G. Meyer, and A. Freimuth, Phys. Rev. B **68**, 140405(R) (2003).
[7] M. Hoinkis, M. Sing, S. Glawion, L. Pisani, R. Valenti, S. van Smaalen, M. Klemm, S. Horn, and R. Claessen, Phys. Rev. B **75**, 245124 (2007).
[8] M. Shaz, S. van Smaalen, L. Palatinus, M. Hoinkis, M. Klemm, S. Horn, and R. Claessen, Phys. Rev. B **71**, 100405(R) (2005).
[9] E. T. Abel, K. Matan, F. C. Chou, E. D. Isaacs, D. E. Moncton, H. Sinn, A. Alatas, and Y. S. Lee, Phys. Rev. B **76**, 214304 (2007).
[10] M. C. Cross and D. S. Fisher, Phys. Rev. B **19**, 402 (1979).
[11] D. B. McWhan, R. M. Fleming, D. E. Moncton, and F. J. DiSalvo, Phys. Rev. Lett. **45**, 269 (1980).
[12] T. M. Rice, Phys. Rev. B **23**, 2413 (1981).
[13] P. Bak, D. Mukamel, J. Villain, and K. Wentowska, Phys. Rev. B **19**, 1610 (1979).
[14] C. Bourbonnais and D. Jerome, in *The Physics of Organic Superconductors and Conductors*, edited by A. Lebed (Springer, Berlin, 2008), p. 357.
[15] K. Ohwada *et al.*, Phys. Rev. Lett. **87**, 086402 (2001).
[16] K. Ohwada *et al.*, Phys. Rev. B **76**, 094113 (2007).
[17] A. R. Goñi, T. Zhou, U. Schwarz, R. K. Kremer, and K. Syassen, Phys. Rev. Lett. **77**, 1079 (1996).
[18] P. H. M. van Loosdrecht, J. Zeman, G. Martinez, G. Dhalenne, and A. Revcolevschi, Phys. Rev. Lett. **78**, 487 (1997).
[19] C. A. Kuntscher, S. Frank, A. Pashkin, M. Hoinkis, M. Klemm, M. Sing, S. Horn, and R. Claessen, Phys. Rev. B **74**, 184402 (2006).
[20] C. A. Kuntscher *et al.*, Phys. Rev. B **78**, 035106 (2008).
[21] M. K. Forthaus, T. Taetz, A. Möller, and M. M. Abd-Elmeguid, Phys. Rev. B **77**, 165121 (2008).
[22] Y.-Z. Zhang, H. O. Jeschke, and R. Valenti, Phys. Rev. Lett. **101**, 136406 (2008).
[23] Y. Feng *et al.*, Phys. Rev. Lett. **99**, 137201 (2007).
[24] R. Jaramillo, Y. Feng, J. C. Lang, Z. Islam, G. Srajer, H. M. Rønnow, P. B. Littlewood, and T. F. Rosenbaum, Phys. Rev. B **77**, 184418 (2008).
[25] R. J. Angel, in *High-Pressure, High-Temperature Crystal Chemistry*, Rev. in Mineral. and Geochem. Vol. 41, edited by R. M. Hazen and R. T. Down (Mineralogical Society of America, Chantilly, VA, 2000), pp. 35–60.
[26] A. Krimmel *et al.*, Phys. Rev. B **73**, 172413 (2006).
[27] D. Mastrogiuseppe, C. Gazza, and A. Dobry, J. Phys.: Condens. Matter **20**, 135223 (2008).
[28] S. Blanco-Canosa, F. Rivadulla, A. Piñeiro, V. Pardo, D. Baldomir, D. I. Khomskii, M. M. Abd-Elmeguid, M. A. López-Quintela, and J. Rivas, Phys. Rev. Lett. **102**, 056406 (2009).